European Radiology (2019) 29:1903–1911
https://doi.org/10.1007/s00330-018-5764-9

ONCOLOGY

PET/CT features discriminate risk of metastasis among single-bone FDG lesions detected in newly diagnosed non-small-cell lung cancer patients

Chae Hong Lim[1] · Tae Ran Ahn[2] · Seung Hwan Moon[1] · Young Seok Cho[1] · Joon Young Choi[1] · Byung-Tae Kim[1] · Kyung-Han Lee[1]

Received: 18 June 2018 / Revised: 9 August 2018 / Accepted: 14 September 2018 / Published online: 12 October 2018

Abstract

Objectives We investigated the capacity of fluorodeoxyglucose (FDG) PET/CT features for stratifying probability of metastasis for single-bone FDG lesions in non-small-cell lung cancer (NSCLC).

Methods Subjects were 118 newly diagnosed NSCLC patients with a solitary bone FDG lesion and no evidence of other distant metastasis based on PET/CT, brain MRI, and contrast-enhanced chest CT. Bone lesion SUV_{max} and CT findings, primary tumor SUV_{max}, clinical T stage, and N stage were analyzed.

Results The bone lesions were determined by biopsy, characteristic MRI findings and clinical follow-up to be metastatic in 33 (28.0%) and benign in 85 cases (72.0%). A cutoff bone SUV_{max} of 4.3 showed good diagnostic performance (81.8% sensitivity, 84.7% specificity, and 83.9% accuracy), but there was considerable overlap. Bone lesion PET/CT features of $SUV_{max} \leq 2$, osteosclerotic rim or fracture correctly diagnosed 20/20 benign, while $SUV_{max} > 10$, soft-tissue mass or bone destruction correctly diagnosed 18/18 metastatic cases. In the remaining 80 cases, bone features of $SUV_{max} > 4.3$ and osteolytic change, and lung tumor features of $SUV_{max} > 6.4$, ≥ T2 stage ($n = 70$), and ≥ N1 stage ($n = 43$) favored metastasis. The presence of one or less of these features correctly diagnosed 38/38 benign, while the presence of four or more features correctly diagnosed 5/5 metastatic cases. The 37 cases with two or three features had either benign ($n = 27$) or metastatic bone disease ($n = 10$).

Conclusion Combining bone lesion and lung tumor PET/CT features can help stratify risk of bone metastasis in these patients.

Key Points

- *In NSCLC with a single-bone FDG lesion, lesion SUV_{max} is useful for differential diagnosis.*
- *CT features of the single-bone FDG lesions provide additional diagnostic value.*
- *High NSCLC SUV_{max}, greater T stage, and FDG positive nodes also favor metastasis.*

Keywords Lung cancer · Positron-emission tomography · Fluorodeoxyglucose · Bone metastasis

Abbreviations

AUC	Area under the curve
FDG	^{18}F-fluorodeoxyglucose
MRI	Magnetic resonance imaging
NSCLC	Non-small-cell lung cancer
PET/CT	Positron-emission tomography/computed tomography
ROC	Receiver operating characteristic
SUV_{max}	Maximum standard uptake value

✉ Kyung-Han Lee
khnm.lee@samsung.com

[1] Department of Nuclear Medicine, Samsung Medical Center, Sungkyunkwan University School of Medicine, 81 Irwon-ro, Gangnam-gu, Seoul 06351, South Korea

[2] Department of Radiology, Samsung Medical Center, Sungkyunkwan University School of Medicine, Seoul 06351, South Korea

Introduction

Lung cancer is the most common cause of cancer-related death worldwide [1]. Non-small-cell lung cancer (NSCLC) most frequently metastasizes to bone [2], occurring in 30–40% of cases [3, 4]. These patients are generally treated with systemic chemotherapy or symptom-based palliative approaches. However, NSCLC metastasis limited to a solitary bone, which occurs in 7% of cases [5], can be treated with more favorable outcome by local treatment such as radiotherapy or surgery [6, 7]. In such cases, a delay of diagnosis may adversely affect clinical outcome [8], and prompt recognition

of bone metastases is important. Indeed, the recently revised TNM staging system takes into account significant differences in survival between single or multiple metastases, separately categorizing these entities as M1b and M1c disease, respectively [9, 10].

Patients newly diagnosed with NSCLC frequently undergo positron-emission tomography/computed tomography (PET/CT) using ^{18}F-fluorodeoxyglucose (FDG) for tumor staging. PET/CT is also useful for detecting skeletal involvement and predicting prognosis in NSCLC patients [11–15], but its diagnostic specificity remains relatively limited. As such, a large portion of bone FDG uptakes turn out to be caused by benign entities. Single-bone FDG lesions, which are commonly detected, are particularly difficult to interpret compared to multiple lesions that make metastatic disease more likely [16]. Bone biopsy can confirm the nature of suspected bone lesions but is invasive, and MRI can aid in bone lesion characterization but at the expense of increased cost and time. It would, therefore, be beneficial to be able to use PET/CT features to stratify single-bone FDG lesions that are likely metastatic and require further investigation and those that may be considered benign and need not delay surgery. Previous studies in cancer patients showed that FDG uptake measurements can help discern bones harboring metastatic disease [17]. Bone site [18] and CT-based anatomical findings [19] might also provide useful diagnostic information. In addition, PET/CT features of the primary tumor associated with rate of metastatic, including FDG avidity [20] and tumor stage [21], could also be useful.

Hence, in this study, we investigated PET/CT features that help characterize the nature of solitary FDG bone lesions in otherwise metastasis-free NSCLC patients at initial staging, and analyzed the ability of these features to differentiate metastatic from benign bone lesions.

Materials and methods

Study population

We retrospectively reviewed medical records of patients who underwent FDG PET/CT for initial staging of newly diagnosed NSCLC at our institute between Jan. 2013 and Dec. 2014. Among these candidates, we selected 140 patients whose PET/CT report described a single bone lesion with focal increased FDG uptake compared to adjacent bones. None of the subjects had evidence of other distant metastasis based on PET/CT, brain MRI, and contrast-enhanced chest CT, which are routinely performed for staging workup of NSCLC patients at our institute. Of these, 6 subjects were excluded because they had history of another prior malignancy, and a total of 134 patients were finally enrolled. Among these, detailed further analysis was performed in 118 cases whose nature of the single-bone FDG lesion was determined using our criteria described below. The remaining 16 cases were excluded from further analysis due to early loss to follow-up without additional tests for final diagnosis. This retrospective study was approved by our Institutional Review Board, and the requirement for written consents was waived.

Final diagnosis of single-bone FDG lesions

Final diagnosis of the single-bone FDG lesions was based on bone biopsy in 11 cases (9.3%). In the remaining 107 cases (90.7%), at least one of the following criteria had to be met for diagnosis of metastasis: (1) magnetic resonance imaging (MRI) including fat-suppressed short tau inversion recovery sequences found to be highly consistent with metastasis by a musculoskeletal radiology specialist with at least 20 years of experience, and (2) disease progression on follow-up PET/CT at sites including the bone-of-interest based on CT-measured size and PET-measured FDG uptake.

Diagnosis of benign bone disease in the absence of biopsy required that none of the above metastasis criteria were met and that clinical and radiologic follow-up was uneventful for at least 1 year.

FDG PET/CT imaging

All patients fasted for at least 6 h and had blood glucose level < 150 mg/ml at the time of PET/CT. Imaging was performed 60 min after injection of 5 MBq/kg FDG without intravenous or oral contrast on a Discovery LS (GE Healthcare; $n = 36$) or a Discovery STe PET/CT scanner (GE Healthcare; $n = 82$). All patients were in a supine position with their arms down. Continuous spiral CT was performed with an 8-slice helical CT (140 keV; 40–120 mA; Discovery LS; $n = 36$) or with 16-slice helical CT (140 keV; 30–170 mA; Discovery STe; $n = 82$). The CT scan data were collected using the following parameters: section width of 5 mm, and table feed of 5 mm per rotation. No intravenous or oral contrast agents were used. An emission scan was then performed from head to thigh for 4 min per frame in 2-D mode with reconstruction of attenuation-corrected PET images ($4.3 \times 4.3 \times 3.9$ mm) using an ordered-subset expectation maximization algorithm (28 subsets, 2 iterations; Discovery LS) or for 2.5 min per frame in 3-D mode with reconstruction of attenuation-corrected PET images ($3.9 \times 3.9 \times 3.3$ mm) using a 3-D ordered-subset expectation maximization algorithm (20 subsets, 2 iterations; Discovery STe).

Analysis of PET/CT images

All PET images were analyzed by a single nuclear medicine physician, who selected transaxial lung tumor and bone lesion slices containing the highest visual FDG uptakes. Spherical volumes-of-interest were manually placed on the lesions using an Advantage Workstation 4.4 (GE Healthcare), and FDG uptakes were measured as the maximum standardized uptake value (SUV_{max}).

The CT portion of PET/CT images were then assessed by a radiologist and a nuclear medicine physician blinded to clinical information using bone and soft-tissue windows. Through consensus, general morphologic features of the bone lesions were categorized as osteolytic, osteoblastic, mixed osteolytic/osteoblastic, or no demonstrable anatomical change. The presence of fracture lines or callus formation was interpreted as fracture. Specific CT findings included presence of an osteosclerotic rim, soft-tissue mass, and bone destruction.

We also evaluated whether PET/CT-based tumor stage of individual patients might help discriminate benign from metastatic bone lesions. Primary lung tumors with the longest diameter < 3 cm on CT without evidence of adjacent organ invasion or satellite nodules were categorized as T1. Lymph nodes with uptake greater than the mediastinum were categorized as FDG positive, unless they were accompanied by calcification or attenuation greater than the aorta.

Statistical analyses

Significance of difference between groups was assessed by Student's *t* tests or Pearson's chi-square tests. Performance was compared by receiver operating characteristic (ROC) curves, and areas under the curve (AUC) were calculated non-parametrically and compared by the method of Hanley and McNeil [22]. Diagnostic sensitivity, specificity, and accuracy were calculated using standard formulas. All calculations were performed with the SPSS (version 23.0; SPSS Inc.) and MedCalc (version 15.5; MedCalc Software) statistical software. $P < 0.05$ was considered significant.

Results

Clinical characteristics of study subjects

Among 134 subjects enrolled, the nature of the single bone lesion was determined using our criteria in 118 cases. These cases underwent further analysis and are therefore the final subjects of this study. Their clinical characteristics are summarized in Table 1. Mean age was 63.0 ± 10.5 years and 70.3% were male. The lung tumor was adenocarcinoma in 71.2% and squamous cell carcinoma in 24.6%. The 16 enrolled cases that were not included for analysis because of undetermined final diagnosis had similar age (65.4 ± 7.2 years), gender (62.5% males), and histologic type (68.8% adenocarcinomas and 31.2% squamous cell carcinomas).

Final diagnosis of single-bone FDG lesions

All of the 118 subjects of our study had a single-bone FDG lesion, leading to a total of 118 lesions. Thirty-three of these lesions (28.0%) were determined to be metastatic by bone biopsy ($n = 8$), highly consistent MRI ($n = 13$), or disease progression on follow-up ($n = 12$). Confirmation of metastasis by bone biopsy included 3 rib lesions, 3 spine lesions, 1 pelvic and 1 long bone lesion. Diagnosis of metastasis by highly consistent MRI included 11 spine and 2 pelvic bone lesions. Diagnosis of metastasis by disease progression included 5 rib lesions, 4 spine lesions, and 1 lesion each in the pelvic bone, sternum, and scapula. Confidence that these lesions represented true metastasis was supported by the fact that all of the patients underwent palliative therapy for bone metastasis.

The remaining 85 bone FDG lesions in our subjects were determined to be benign. In 78 cases, this was based on follow-up PET/CT, bone scintigraphy, MRI, or CT that demonstrated no findings of disease progression at the bone site for more than 1 year (31.0 ± 12.7 months; range, 13 to 56 months). In the remaining 7 cases, diagnosis of benignity was based on the absence of symptom/signs suggesting bone metastasis for at least 20 months of clinical follow-up, although follow-up imaging of the bone-of-interest was not done (38.7 ± 12.4 months; range, 20 to 54 months). Subjects with metastatic and benign single-bone FDG lesions were not different in age, gender, or primary tumor histologic type.

Lesion site does not help differentiate metastatic from benign single bone lesions

The distribution of the single-bone FDG lesions in our subjects is shown in Table 2. Lesion site was most frequently the spine (54.2%), followed by ribs (22.0%) and pelvic bone (11.9%). Similarly, metastatic disease was most frequently found in the spine (54.6%), followed by rib (24.2%) and pelvic bone (12.1%). The rate of metastasis was 28.1% for spine, 30.8% for rib, 28.6% for pelvis, and 11.1% for long bone. Among other sites, 1 of 4 scapular lesions and 1 of 1 sternal lesion were found to be metastatic. Overall, these findings demonstrate that lesion site does not help differentiate metastatic from benign bone lesions.

PET features that help differentiate metastatic from benign bone disease

When FDG uptake of the bone lesions was measured, SUV_{max} was clearly greater for metastatic compared to

Table 1 Characteristics of 118 NSCLC patients with a single-bone FDG lesion on PET/CT

	Total ($n = 118$)	Metastasis ($n = 33$)	Benign ($n = 85$)	p
Age (year; mean ± SD)	63.0 ± 10.5	64.6 ± 10.1	62.4 ± 10.6	0.299*
Male gender	83 (70.3%)	22 (66.7%)	61 (71.8%)	0.586†
Histologic profile				0.256†
Adenocarcinoma	84 (71.2%)	26 (78.8%)	58 (68.2%)	
Non-adenocarcinoma	34 (28.8%)	7 (21.2%)	27 (31.8%)	
Clinical PET stage				
T stage (T1 vs. T2–4)	48 vs.70	7 vs. 26	41 vs. 44	0.007†
N stage (N0 vs. N1–3)	75 vs. 43	10 vs. 23	65 vs. 20	0.000†
Bone SUV_{max} (mean ± SD)	4.8 ± 3.8	8.4 ± 5.5	3.5 ± 1.3	0.000*
Primary SUV_{max} (mean ± SD)	8.1 ± 6.0	10.8 ± 6.8	7.0 ± 5.4	0.002*

NSCLC non-small-cell lung cancer, *SUV_{max}* maximum standard uptake value, *vs.* versus

**t* test;

† Pearson's chi-square test

benign disease (8.4 ± 5.5 vs. 3.5 ± 1.3, $p < 0.001$; Fig. 1a). All 9 bone lesions with $SUV_{max} > 10.0$ were metastatic, and all 7 bone lesions with $SUV_{max} \leq 2.0$ were benign. The remaining 102 bone lesions with SUV_{max} between 2.0 and 10.0 could be either benign or metastatic. In particular, benign fractures could show SUV_{max} levels of up to 9.8 and 8.5, respectively, for rib and spine lesions. On the other hand, there were 4 metastatic bone lesions with low SUV_{max} between 2.0 and 3.0.

ROC analysis of bone lesion SUV_{max} showed an AUC of 0.853 (95% CI, 0.78–0.91; Fig. 1b). The best cutoff SUV_{max} of 4.3 correctly identified 27/33 metastatic and 72/85 benign lesions, yielding 81.8% sensitivity, 84.7% specificity, and 83.9% accuracy. This level of performance was maintained throughout different bone lesion sites, except for the ribs (62.5% sensitivity and 72.2% specificity). $SUV_{max} > 4.3$ of pelvic bone lesions showed high specificity (100%) but low specificity (50%) for metastasis (Table 2). Interestingly, the diagnostic performance of $SUV_{max} > 4.3$ was different according to primary tumor histology. Hence, sensitivity (85.2%), specificity (96.3%), and accuracy (94.1%) were higher for non-adenocarcinoma compared to adenocarcinoma (76.2%, 81.0%, and 75.0%, respectively; Table 2). Overall, however, differential diagnosis based on SUV_{max} alone was associated with a significant number of misdiagnosed cases. A representative case with benign bone disease despite a high SUV_{max} and another case with metastatic bone disease despite a low SUV_{max} are illustrated in Figs. 2 and 3, respectively.

Interestingly, the SUV_{max} of the primary lung tumor was also significantly greater for patients whose bone lesions were metastatic compared to benign (10.8 ± 6.8 vs. 7.0 ± 5.4; $p < 0.002$). ROC analysis of lung tumor SUV_{max} performance for distinguishing metastasis showed an AUC of 0.677 (95% CI, 0.59–0.76). The best cutoff SUV_{max} of 6.4

Table 2 Diagnostic accuracy of SUV_{max} cutoff according to lesion site and tumor histology

Lesion	Metastatic (%)	TP	TN	FP	FN	SN (%)	SP (%)	Accuracy (%)
Total	33/118 (28.0%)	27	72	13	6	81.8	84.7	83.9
Lesion site								
Spine	18/64 (28.1%)	17	40	6	1	94.4	87.0	89.1
Rib	8/26 (30.8%)	5	13	5	3	62.5	72.2	69.2
Pelvis	4/14 (28.6%)	2	10	0	2	50.0	100.0	85.7
Long bone	1/9 (11.1%)	1	7	1	0	100.0	87.5	88.9
Others*	2/5 (40.0%)	2	2	1	0	100.0	66.7	80.0
Tumor histology								
ADC	26/84 (31.0%)	16	47	11	5	76.2	81.0	75.0
Non-ADC	7/34 (20.6%)	6	26	1	1	85.7	96.3	94.1

TP true positive, *TN* true negative, *FP* false positive, *FN* false negative, *SN* sensitivity, *SP* specificity, *ADC* adenocarcinoma

*Includes scapula and sternum

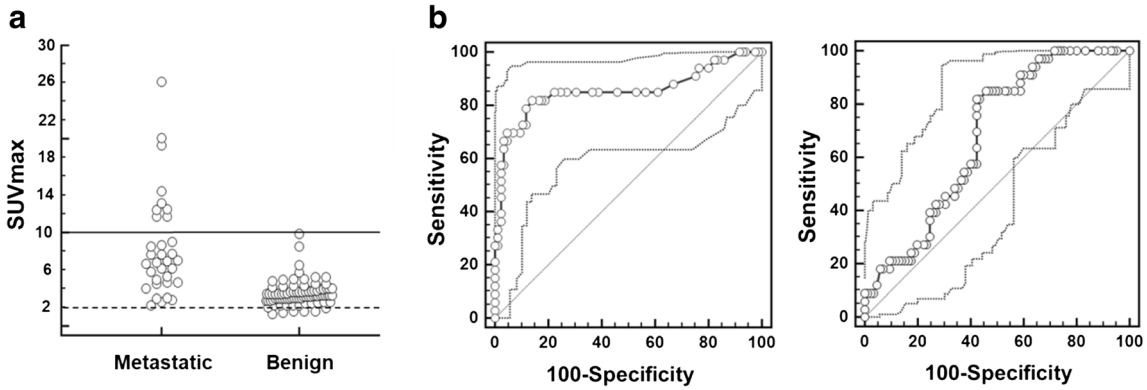

Fig. 1 FDG uptake levels of single-bone FDG lesions and primary lung tumors in 118 patients. **a** Dot plot depicting SUV_{max} of single-bone FDG lesions. All bone lesions with $SUV_{max} \leq 2$ (dashed line) were benign, whereas all with $SUV_{max} > 10$ (solid line) were metastatic. On the other hand, SUV_{max} between 2 and 10 lacked sufficient specificity for differential diagnosis. **b** ROC curve illustrating performance of bone lesion SUV_{max} (left) and primary lung tumor SUV_{max} (right) for discerning benign and metastatic single bone lesions. Dotted lines indicate upper and lower limit of 95% confidence intervals

yielded 81.8% sensitivity, 57.7% specificity, and 64.4% accuracy (Fig. 1b). This was in itself insufficient performance, but we found that lower SUV_{max} (≤ 4.3) bone lesions in patients with higher SUV_{max} (> 6.4) lung tumors were significantly more likely to be benign (32/37) compared to their counterpart (52/81; $p = 0.018$). This indicated that primary lung tumor SUV_{max} could be a useful PET feature for bone FDG lesion differentiation.

In addition, the presence of FDG-positive thoracic lymph nodes was also associated with a significantly greater likelihood that the single bone lesion was metastatic compared to their absence, indicating their potential usefulness for bone lesion differentiation.

CT features of single bone lesions useful for differential diagnosis

We next assessed CT features of the bone FDG lesion that could offer useful information for differential diagnosis. The results showed that metastasis was favored by the presence of osteolytic change (16/19, 84.2%; $p = 0.000$), soft-tissue mass (11/11, 100%; $p = 0.000$), or bone destruction (15/15, 100%; $p = 0.000$; Table 3). Conversely, benign disease was favored by the presence of fracture (9/9, 100%; $p = 0.060$) or osteosclerotic rim (7/7, 100%; $p = 0.188$; Table 3).

A CT feature of the primary lung cancer that was helpful was T2-T4 tumor stage, which was significantly more likely

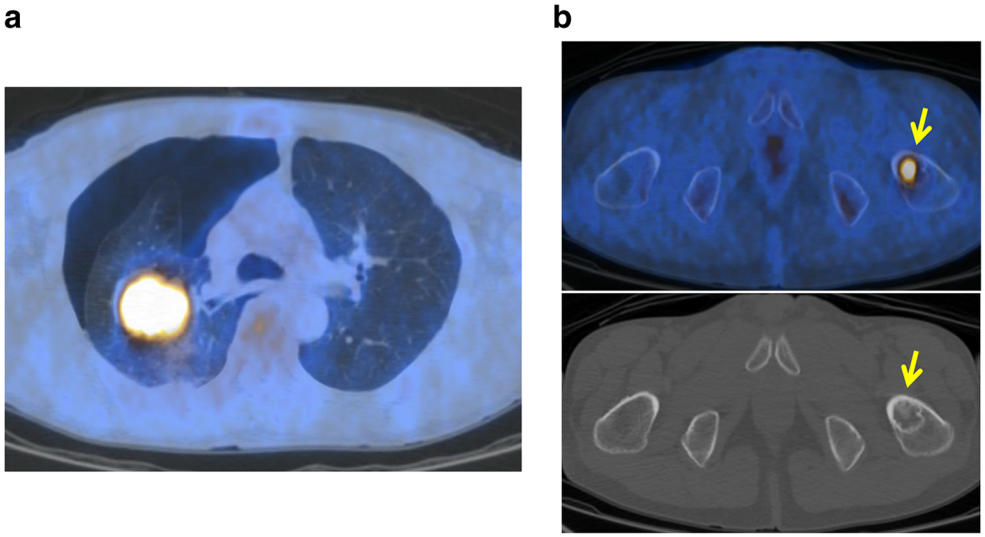

Fig. 2 Fusion PET/CT features of a 48-year old man with adenocarcinoma. **a** Initial PET/CT (transaxial) demonstrated a 4.4-cm right upper lobe mass with high FDG uptake ($SUV_{max} = 8.1$). **b** A transaxial slice at the hip level showed a discrete single bone lesion in the left proximal femur with high FDG uptake ($SUV_{max} = 5.2$) that suggested metastasis (top, arrow). However, the CT portion of the PET/CT images demonstrated osteoblastic bone change with a peripheral sclerotic rim, which indicated benign bone disease (bottom, arrow). Bone biopsy confirmed this lesion to harbor benign reactive bone formation

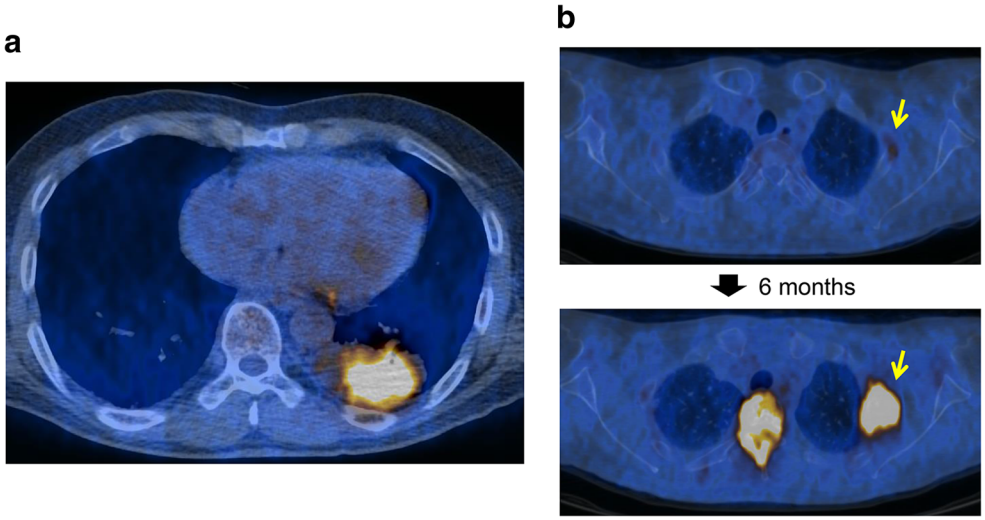

Fig. 3 Fusion PET/CT features of a 63-year-old man with adenocarcinoma. **a** Initial PET/CT (transaxial) demonstrated an 8-cm left lower lobe mass with high FDG uptake ($SUV_{max} = 7.0$). **b** A PET/CT slice at a higher level showed a discrete focus of low FDG uptake ($SUV_{max} = 2.2$) in the left second rib that was unaccompanied by bone change on CT images (top, arrow). Follow-up PET/CT 6 months after receiving curative lobectomy without further evaluation, the rib lesion showed disease progression, revealing that it had been metastatic (bottom, arrow)

to be associated with metastatic bone lesion compared to T1 tumor stage.

Proposed diagnostic flow to combine PET/CT features for differential diagnosis

Finally, we reclassified each single-bone FDG lesion using PET/CT features found useful for differential diagnosis (Fig. 4). Metastasis-specific bone lesion features of $SUV_{max} > 10.0$, soft-tissue mass formation, or bone destruction correctly diagnosed metastasis in 18 lesions. Benignity-specific bone lesion features of $SUV_{max} \leq 2.0$, fracture, or osteosclerotic rim correctly diagnosed no metastasis in 20 lesions. The case illustrated in Fig. 2 showed a single bone lesion in the proximal femur that had high FDG uptake ($SUV_{max} = 5.2$) but could be correctly classified as benign by the presence of a discrete osteosclerotic rim.

The remaining 79 cases were evaluated for number of features favoring metastasis; i.e., bone lesion $SUV_{max} > 4.3$, lung tumor $SUV_{max} > 6.4$, clinical T stage ≥ T2, FDG-positive lymph nodes, and osteolytic bone change. Among cases of this group, all 38 subjects with one or less of these features could be correctly diagnosed as having benign bone disease, and all 5 subjects with 4 or more features could be correctly diagnosed as having bone metastasis. The remaining 37 subjects had two or three features and were found to have either benign ($n = 27$) or metastatic bone disease ($n = 10$). The case illustrated in Fig. 3 showed a single-rib lesion that had a low SUV_{max} of only 2.2, which might be easily interpreted as benign. However, there were no benignity-specific PET/CT features whereas there were two metastasis-favoring features, and the lesion was later found to be metastatic.

Table 3 Metastasis rate according to CT features of 118 single-bone FDG lesions

Bone lesion site	Total	Metastasis	Benign	*p*
General feature				
Osteolytic change	19 (16.1%)	16 (48.5%)	3 (3.5%)	0.000†
Osteoblastic change	33 (28.0%)	5 (15.2%)	28 (32.9%)	0.068*
Mixed change	13 (11.0%)	4 (12.4%)	9 (10.6%)	0.755†
No change	44 (37.3%)	8 (24.2%)	36 (42.4%)	0.068*
Fracture	9 (7.6%)	0 (0.0%)	9 (10.6%)	0.060†
Specific feature				
Osteosclerotic rim	7 (5.9%)	0 (0.0%)	7 (8.2%)	0.188†
Soft-tissue mass	11 (9.3%)	11 (33.3%)	0 (0.0%)	0.000†
Bone destruction	15 (12.7%)	15 (45.5%)	0 (0.0%)	0.000†

*Pearson's chi-square test
† Fisher's exact test

Discussion

In this study, we evaluated patients with newly diagnosed NSCLC to investigate the usefulness of PET/CT features to differentiate single-bone FDG lesions caused by metastasis from benign causes. The final diagnosis was determined by bone biopsy or clinical follow-up with imaging studies including bone scintigraphy, CT, PET/CT, and MRI. Although bone scintigraphy has low sensitivity for lytic bone metastases, it has been reported to have a high sensitivity of 87% for detecting metastasis [12]. Furthermore, the use of multiple imaging techniques

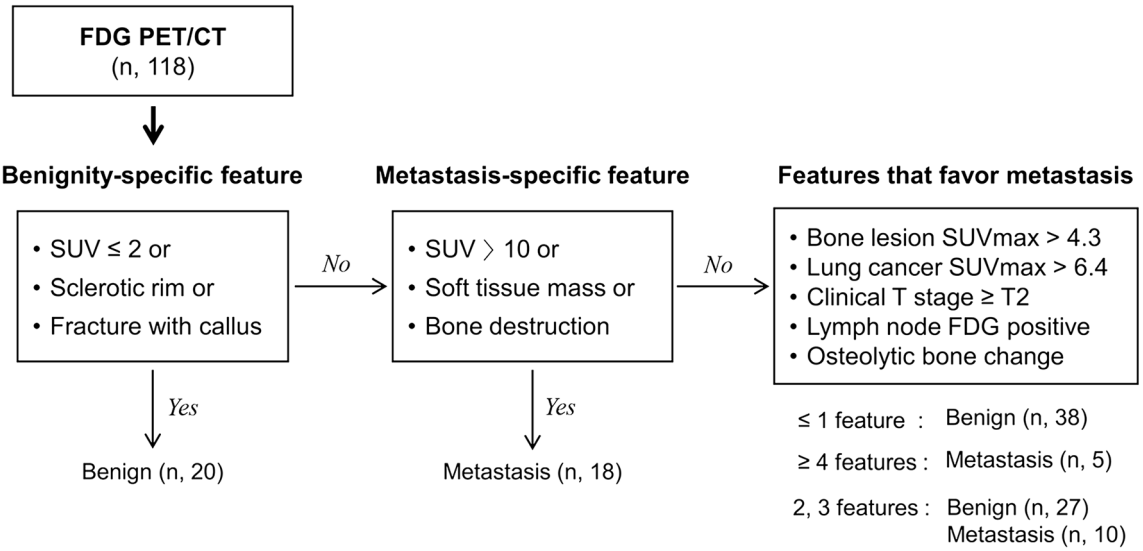

Fig. 4 Flowchart for differential diagnosis of single-bone FDG lesions in 118 newly diagnosed NSCLC patients. Using this method, PET/CT features correctly recognized 25 metastatic and 56 benign bone lesions. Only 37 bone lesions remained that required further evaluation for differentiation

compensated for the limitations of each modality alone. The final diagnosis thus reached showed that only 28% of the bone lesions in our population were metastatic. This verifies the limited cost-effectiveness to perform bone biopsy or MRI for all such lesions. Our study demonstrates that PET/CT features can help assess the risk of metastatic disease and stratify patients that require further evaluation of the bone lesion and those that can undergo treatment of the lung cancer without delay.

The first clue we looked at was bone site. In our subjects, FDG bone lesions that were metastatic occurred most frequently in the spine, followed by the ribs and pelvis. This is consistent with the pattern of bone metastasis for NSCLC patients previously reported by Sugiura et al [8] and more recently by Zhou et al [23]. However, benign bone lesions in our subjects occurred in a rather similar distribution. Thus, bone site was not useful for discerning the nature of single bone lesions.

Lesion SUV_{max} has been proposed useful for separating malignant from benign disease. In our subjects, a cutoff SUV_{max} of 4.3 provided relatively good sensitivity and specificity for discerning bone metastasis. This level of accuracy was maintained for lesions of all bone sites, except for rib lesions that showed 69.2% accuracy. Based on SUV_{max}, there were 5 false positive rib lesions. Two rib fractures had SUV_{max} levels exceeding 4.5, which is consistent with previous reports of rib fractures with high FDG uptake that can be mistaken for metastatic disease [24]. Vertebral compression fracture was also a benign cause for high bone lesion SUV_{max}.

Although bone lesion SUV_{max} displayed relatively good diagnostic performance in our study, it is well known that moderate SUV_{max} levels have limited value for lesion characterization. This is because many benign causes including granulomatous and inflammatory lesions can also take up FDG in levels that overlap considerably with those of malignant tumors. In the bone, healing fractures and histiocytic or giant cell-containing benign lesions can have increased FDG uptake that mimics osseous metastasis [25, 26]. Therefore, it should be noted that the SUV_{max} threshold suggested by this study as well as by previous studies [27] actually have limited differential power for discerning malignant from benign bone lesions. Our results further indicate that caution is required for interpreting rib lesions as well as interpreting single bone lesions of lung adenocarcinoma patients based on bone lesion SUV_{max}, which showed lower diagnostic performance. The latter is likely contributed by the known lower FDG avidity of lung adenocarcinoma cells [28, 29].

Overall, using a cutoff bone lesion SUV_{max} of 4.3 alone would have misclassified 6 metastatic lesions as benign (Fig. 4). Alternatively, using SUV_{max} thresholds of > 10.0 and ≤ 2.0, respectively, could discern metastatic and benign bone lesions in a perfect manner. This left 102 bone lesions that required additional PET/CT features to aid in differential diagnosis.

Additional information useful for lesion characterization can be provided by the CT portion of PET/CT studies. For example, Strobel et al found that CT findings were useful for recognizing FDG-avid bone lesions caused by benign fibrous dysplasia or aneurysmal bone cysts [30]. We also observed CT features that could add diagnostic value over SUV measurements alone. First, the presence of soft-tissue mass formation or bone destruction was characteristic of metastatic disease. The feature of osteolytic change also significantly favored metastasis, although it was also shown in some benign lesions. On the other hand, the presence of an osteosclerotic rim or fracture characterized benignity, as previously described [24, 31]. Interpreting these CT features as signs of benignity

regardless of FDG avidity reduced the number of false positive cases compared to using SUV_{max} alone. Although bone lesion size is also an interesting potential factor to consider, this was not included for analysis in this study because a considerable number of bone lesions were not accompanied by measurable anatomic change. Furthermore, the non-enhanced CT portion of PET/CT images is not ideal for measuring bone lesion size, while MRI was performed in only a portion of our subjects ($n = 23$).

In addition to bone lesion features, PET/CT can also assess primary tumor and lymph node features related to the probability of distant metastasis, including tumor stage and FDG avidity that represent cancer aggressiveness. A previous study reported that primary tumor SUV correlates with presence of distant metastases in a manner independent of tumor size [32]. Another study in patients with T1-stage NSCLC suggested primary tumor FDG uptake as a potential indicator of distant metastasis [33]. This is not surprising since increased FDG uptake in lung cancer represents heightened metabolic activity that is strongly associated with tumor aggressiveness and lymphovascular invasion, early steps necessary for nodal and distant metastasis [34–36]. Furthermore FDG uptake of lymph nodes is also known to correlate with distant metastasis [37]. In our study, we confirmed that greater lung cancer FDG uptake, higher clinical T stage, and FDG-positive lymph nodes were associated with greater likelihood metastatic bone disease. In patients with primary lung tumors with high FDG uptake, bone lesions could be metastatic even at T1 and N0 stage. In these patients, however, bone lesions with low FDG uptake were not likely to be metastatic.

We finally stratified the probability of metastasis for single FDG bone lesions using SUV_{max} (> 10.0 or ≤ 2.0) in combination with other PET/CT features. CT features including soft-tissue mass formation, bone destruction, fracture, and osteosclerotic rim correctly classified 18 metastatic and 20 benign lesions. In the remaining patients, five PET/CT features that significantly favored bone metastasis were higher bone lesion SUV_{max}, higher lung tumor SUV_{max}, greater T2 stage, FDG-positive intrathoracic lymph nodes, and osteolytic bone change. Of these, bone FDG lesions with one or less of these features were all benign, and those with four or more of these features were all metastatic. Finally, only 37 bone lesions had two or three of these features and required further examination because they could be either metastatic or benign.

A limitation of our study is its retrospective design. Final diagnosis was based not only on biopsy but also on imaging studies and clinical follow-up. However, all bone lesions determined to be metastatic by MRI were evaluated by a full series of imaging sequences including fat-suppressed short tau inversion recovery that is recognized to have high diagnostic accuracy [38, 39]. Furthermore, all of these patients were clinically judged by their attending physician to have metastatic disease in the bone-of-interest and underwent palliative treatment. As for the diagnosis of benignity, our criteria of 1 year or more of uneventful follow-up is widely considered sufficient evidence. Finally, the use of two different PET/CT scanners is a potential source for instrumentation variability. However, we confirmed that there was no difference ($p = 0.980$) of mean bone lesion SUV_{max} between subjects imaged by LS (SUV_{max}, 4.8 ± 3.3) and STe scanners (SUV_{max}, 4.8 ± 4.0).

Conclusions

Single-bone FDG lesions detected by PET/CT in newly diagnosed NSCLC patients can be difficult to interpret. This study demonstrates that bone lesion SUV_{max} helps discern metastasis from benign disease, but with significant overlap remaining. Combining other PET/CT features of the bone lesion and lung tumor provides additional diagnostic value over SUV_{max} measurements alone, which can be used to stratify patients likely to harbor bone metastasis and those with benign bone conditions.

Funding This study was supported by the Basic Science Research Program through the National Research Foundation of Korea (NRF) funded by the Ministry of Science, ICT, and Future Planning (NRF-2015R1A2A2A01006419 and 2016R1C1B2013411).

Compliance with ethical standards

Guarantor The scientific guarantor of this publication is Kyung-Han Lee.

Conflict of interest The authors of this manuscript declare no relationships with any companies, whose products or services may be related to the subject matter of the article.

Statistics and biometry No complex statistical methods were necessary for this paper.

Informed consent Written informed consent was waived by the Institutional Review Board.

Ethical approval Institutional Review Board approval was obtained.

Methodology
- Retrospective
- Diagnostic or prognostic study
- Performed at one institution

References

1. Torre LA, Bray F, Siegel RL, Ferlay J, Lortet-Tieulent J, Jemal A (2015) Global cancer statistics, 2012. CA Cancer J Clin 65:87–108
2. Coleman RE (2006) Clinical features of metastatic bone disease and risk of skeletal morbidity. Clin Cancer Res 12:6243s–6249s

3. Tsuya A, Kurata T, Tamura K, Fukuoka M (2007) Skeletal metastases in non-small cell lung cancer: a retrospective study. Lung Cancer 57:229–232
4. Al Husaini H, Wheatley-Price P, Clemons M, Shepherd FA (2009) Prevention and management of bone metastases in lung cancer: a review. J Thorac Oncol 4:251–259
5. Pfannschmidt J, Dienemann H (2010) Surgical treatment of oligometastatic non-small cell lung cancer. Lung Cancer 69:251–258
6. Zhao T, Gao Z, Wu W, He W, Yang YI (2016) Effect of synchronous solitary bone metastasectomy and lung cancer resection on non-small cell lung cancer patients. Oncol Lett 11:2266–2270
7. Komatsu T, Kunieda E, Oizumi Y, Tamai Y, Akiba T (2012) An analysis of the survival rate after radiotherapy in lung cancer patients with bone metastasis: is there an optimal subgroup to be treated with high-dose radiation therapy? Neoplasma 59:650–657
8. Sugiura H, Yamada K, Sugiura T, Hida T, Mitsudomi T (2008) Predictors of survival in patients with bone metastasis of lung cancer. Clin Orthop Relat Res 466:729–736
9. Kay FU, Kandathil A, Batra K, Saboo SS, Abbara S, Rajiah P (2017) Revisions to the tumor, node, metastasis staging of lung cancer (8th edition): rationale, radiologic findings and clinical implications. World J Radiol 9:269–279
10. Detterbeck FC, Boffa DJ, Kim AW, Tanoue LT (2017) The eighth edition lung cancer stage classification. Chest 151:193–203
11. Bury T, Barreto A, Daenen F, Barthelemy N, Ghaye B, Rigo P (1998) Fluorine-18 deoxyglucose positron emission tomography for the detection of bone metastases in patients with non-small cell lung cancer. Eur J Nucl Med 25:1244–1247
12. Qu X, Huang X, Yan W, Wu L, Dai K (2012) A meta-analysis of ^{18}FDG-PET-CT, ^{18}FDG-PET, MRI and bone scintigraphy for diagnosis of bone metastases in patients with lung cancer. Eur J Radiol 81:1007–1015
13. Cheran SK, Herndon JE 2nd, Patz EF Jr (2004) Comparison of whole-body FDG-PET to bone scan for detection of bone metastases in patients with a new diagnosis of lung cancer. Lung Cancer 44:317–325
14. Lee SM, Goo JM, Park CM et al (2016) Preoperative staging of non-small cell lung cancer: prospective comparison of PET/MR and PET/CT. Eur Radiol 26:3850–3857
15. Lee JW, Seo KH, Kim ES, Lee SM (2017) The role of ^{18}F-fluorodeoxyglucose uptake of bone marrow on PET/CT in predicting clinical outcomes in non-small cell lung cancer patients treated with chemoradiotherapy. Eur Radiol 27:1912–1921
16. Wu PS, Chiu NT, Lee BF, Yao WJ, W Chen HH (2002) Clinical significance of solitary rib hot spots on bone scans in patients with extraskeletal cancer: correlation with other clinical manifestations. Clin Nucl Med 27:567–571
17. Hur J, Yoon CS, Ryu YH, Yun MJ, Suh JS (2007) Accuracy of fluorodeoxyglucose-positron emission tomography for diagnosis of single bone metastasis: comparison with bone scintigraphy. J Comput Assist Tomogr 31:812–819
18. Jacobson AF, Stomper PC, Jochelson MS, Ascoli DM, Henderson IC, Kaplan WD (1990) Association between number and sites of new bone scan abnormalities and presence of skeletal metastases in patients with breast cancer. J Nucl Med 31:387–392
19. Nakamoto Y, Cohade C, Tatsumi M, Hammoud D, Wahl RL (2005) CT appearance of bone metastases detected with FDG PET as part of the same PET/CT examination. Radiology 237:627–634
20. Zhu SH, Zhang Y, Yu YH et al (2013) FDG PET-CT in non-small cell lung cancer: relationship between primary tumor FDG uptake and extensional or metastatic potential. Asian Pac J Cancer Prev 14:2925–2929
21. Quint LE, Tummala S, Brisson LJ et al (1996) Distribution of distant metastases from newly diagnosed non-small cell lung cancer. Ann Thorac Surg 62:246–250
22. Hanley JA, McNeil BJ (1983) A method of comparing the areas under receiver operating characteristic curves derived from the same cases. Radiology 148:839–843
23. Zhou Y, Yu QF, Peng AF, Tong WL, Liu JM, Liu ZL (2017) The risk factors of bone metastases in patients with lung cancer. Sci Rep 7:8970
24. Choi HS, Yoo IeR, Park HL, Choi EK, Kim SH, Lee WH (2014) Role of ^{18}FDG-PET/CT in differentiation of a benign lesion and metastasis on the ribs of cancer patients. Clin Imaging 38:109–114
25. Meyer M, Gast T, Raja S, Hubner K (1994) Increased F-18 FDG accumulation in an acute fracture. Clin Nucl Med 19:13–14
26. Aoki J, Watanabe H, Shinozaki T et al (2001) FDG PET of primary benign and malignant bone tumors: standardized uptake value in 52 lesions. Radiology 219:774–777
27. Shin DS, Shon OJ, Byun SJ, Choi JH, Chun KA, Cho IH (2008) Differentiation between malignant and benign pathologic fractures with F-18-fluoro-2-deoxy-D-glucose positron emission tomography/computed tomography. Skeletal Radiol 37:415–421
28. Aquino SL, Halpern EF, Kuester LB, Fischman AJ (2007) FDG-PET and CT features of non-small cell lung cancer based on tumor type. Int J Mol Med 19:495–499
29. de Geus-Oei LF, van Krieken JH, Aliredjo RP et al (2007) Biological correlates of FDG uptake in non-small cell lung cancer. Lung Cancer 55:79–87
30. Strobel K, Exner UE, Stumpe KD et al (2008) The additional value of CT images interpretation in the differential diagnosis of benign vs. malignant primary bone lesions with 18F-FDG-PET/CT. Eur J Nucl Med Mol Imaging 35:2000–2008
31. Costelloe CM, Chuang HH, Madewell JE (2014) FDG PET/CT of primary bone tumors. AJR Am J Roentgenol 202:W521–W531
32. Sachs S, Bilfinger TV, Komaroff E, Franceschi D (2005) Increased standardized uptake value in the primary lesion predicts nodal or distant metastases at presentation in lung cancer. Clin Lung Cancer 6:310–313
33. Li M, Liu N, Hu M et al (2009) Relationship between primary tumor fluorodeoxyglucose uptake and nodal or distant metastases at presentation in T1 stage non-small cell lung cancer. Lung Cancer 63:383–386
34. Higashi K, Ueda Y, Ayabe K et al (2000) FDG PET in the evaluation of the aggressiveness of pulmonary adenocarcinoma: correlation with histopathological features. Nucl Med Commun 21:707–714
35. Duhaylongsod FG, Lowe VJ, Patz EF Jr, Vaughn AL, Coleman RE, Wolfe WG (1995) Lung tumor growth correlates with glucose metabolism measured by fluoride-18 fluorodeoxyglucose positron emission tomography. Ann Thorac Surg 60:1348–1352
36. Higashi K, Ito K, Hiramatsu Y et al (2005) 18F-FDG uptake by primary tumor as a predictor of intratumoral lymphatic vessel invasion and lymph node involvement in non-small cell lung cancer: analysis of a multicenter study. J Nucl Med 46:267–273
37. Cho H, Kim SH, Kim H et al (2018) Lymph node with the highest FDG uptake predicts distant metastasis-free survival in patients with locally advanced nasopharyngeal carcinoma. Clin Nucl Med 43:e220–e225
38. Walker R, Kessar P, Blanchard R et al (2000) Turbo STIR magnetic resonance imaging as a whole-body screening tool for metastases in patients with breast carcinoma: preliminary clinical experience. J Magn Reson Imaging 11:343–350
39. Mehta RC, Marks MP, Hinks RS, Glover GH, Enzmann DR (1995) MR evaluation of vertebral metastases: T1-weighted, short-inversion-time inversion recovery, fast spin-echo, and inversion-recovery fast spin-echo sequences. AJNR Am J Neuroradiol 16:281–288